

OECD MCCI Project
Small-Scale Water Ingression and Crust Strength Tests (SSWICS)
SSWICS-10 Test Data Report: Thermal Hydraulic Results

Rev. 1 - FINAL

March, 2008

by:

S. Lomperski, M. T. Farmer, D. Kilsdonk, R. Aeschlimann

Nuclear Engineering Division
Argonne National Laboratory
9700 S. Cass Avenue
Argonne, IL 60439
USA

Table of Contents

1. Introduction..... 1

2. System Description..... 1

 2.1 Test Apparatus 1

 2.2 Instrumentation 2

3. Test Parameters and Course of Test 8

4. Sensor Malfunctions and Abnormalities 9

5. Data Reduction..... 9

List of Plots

A.1 Temperatures at bottom of melt..... 13

A.2 Temperatures of selected steel structures..... 13

A.3 Total pressure in reaction vessel and position of valve V-quench..... 14

A.4 Condensate tank inventory as measured by ΔP and level sensors 14

A.5 Water injection into RV and HX secondary side flow rate..... 15

A.6 Integrated quench flow and calculated RV liquid inventory 15

A.7 Secondary side fluid temperature at HX inlet and outlet 16

A.8 Miscellaneous gas and fluid temperatures 16

A.9 Fluid temperatures in the condensate tank..... 17

A.10 Heat flux at corium surface based on mass and energy balances 17

1. Introduction

The Melt Attack and Coolability Experiments (MACE) program at Argonne National Laboratory addressed the issue of the ability of water to cool and thermally stabilize a molten core/concrete interaction (MCCI) when the reactants are flooded from above. These experiments provided unique, and for the most part repeatable, indications of heat transfer mechanisms that could provide long term debris cooling. However, the results did not demonstrate definitively that a melt would always be completely quenched. This was due at least partially to the fact that the crust anchored to the test section sidewalls in every test, which led to melt/crust separation, even at the largest test section lateral span of 1.2 m. This decoupling is not expected for a typical reactor cavity where the lateral span is much larger, ~5-6 m. Instead, the crust is expected to fracture under the weight of the coolant and the crust itself so that coolant contact with the melt is maintained. However, because of a lack of knowledge of the strength of the crust, one cannot be certain that it would actually fracture under such circumstances.

As part of the MCCI-1 and MCCI-2 programs, a series of separate-effects experiments has been conducted to measure corium quench rates and crust strength to investigate the various debris cooling mechanisms identified in the MACE program. Each quench test involved cooling a molten mass of UO_2 , ZrO_2 , and concrete constituents, which produced a corium ingot that was later load tested to determine its mechanical strength. The quench tests were designed to optimize measurements of heat flux from the corium surface and consequently the ingots that were formed were not of optimal thickness for the strength measurements.

For the quench tests, a minimum corium depth of 150 mm was deemed necessary to obtain a satisfactory heat flux measurement. However, 150 mm is too much for optimal load testing and so the ingots were sectioned (cut in the radial direction) to increase their aspect ratio (diameter/thickness) to make them more suitable for load testing. Unfortunately, the cutting process is laborious and involves much handling of the ingot and therefore decreases the certainty that the mechanical strength of the sections is close to that of the original ingot. This uncertainty would be eliminated if the ingots produced by the quench tests could be tested without having to cut them.

SSWICS-9 & 10, in contrast to previous tests, are designed to optimize the ingot for load testing. A reduced amount of corium will be used in the quench test to produce a thinner ingot. The ingot will then be load tested without sectioning. This report details the results of the SSWICS-10 quench test.

2. System Description

2.1 Test Apparatus

The SSWICS reaction vessel (RV) has been designed to hold up to 100 kg of melt at an initial temperature of 2500°C. The RV lower plenum consists of a 67.3 cm long, 45.7 cm (18") outer diameter carbon steel pipe (Fig. 2.1). The pipe is insulated from the melt by a 6.4 cm thick layer of cast MgO, which is called the "liner". The selected pipe and insulation dimensions result in a melt diameter of about 30 cm and a surface area of 707 cm². The melt depth at the maximum charge of 100 kg is about 20 cm.

The RV lower flange is insulated with a 6.4 cm thick slab of cast MgO (the “basemat”) that spans the entire inner diameter of the pipe. The basemat and liner form the crucible containing the corium. A 2-mm thick layer of ZrO₂ felt covers the basemat to absorb the initial thermal shock of thermite ignition. The felt, in turn, is covered with a 0.25 mm thick tungsten plate to ensure that the corium does not adhere to the basemat. This particular geometry was chosen to facilitate removal of the basemat for the crust strength measurement tests. Corium has a tendency to bond with the MgO insulation and this design allows one to detach the basemat from the liner without damaging the crust.

The RV upper plenum consists of a second section of pipe with a stainless steel protective liner. Three 10 cm pipes welded near the top of the vessel provide 1) a vent line for the initial surge of hot noncondensable gases generated by the thermite reaction, 2) a pressure relief line with a rupture disk (7.7 bar at 100°C), and 3) an instrument flange for the absolute pressure transmitter that measures the reaction vessel pressure. Four 6 mm (¼”) tubes serve as water inlets for melt quenching. A baffle is mounted below the upper flange and the water flow is directed towards the baffle to reduce the momentum of the fluid before it drops down onto the melt. The baffle is also intended to prevent water droplets from being carried up towards the condenser, which would adversely affect the heat flux measurement. A fourth 10 cm pipe welded to the top flange provides an outlet to carry steam from the quenching melt to four cooling coils. The water-cooled coils condense the steam, which is collected within a 200 cm high, 20 cm diameter condensate tank (CT). Figure 2.2 is a schematic that provides an overview of the entire SSWICS melt-quench facility.

Some differences between this configuration and that of earlier tests:

- Sand is not added to the 5 mm gap to reduce lateral heat transfer. The melt is so thin and the surface to volume ratio so high that the presence of the sand would have little effect on the melt cooling rate
- The ZrO₂ felt over the basemat replaces the thicker cast ZrO₂ used in all previous tests. The basemat requires less thermal shock protection from the smaller melt
- The lower MgO liner has been reduced in height by a factor of two because of the lower melt inventory
- Some of the consumable instruments were omitted (detailed in next section)

2.2 Instrumentation

The melt mass is only ⅓ that of previous quench tests since it has been optimized for subsequent measurements of mechanical strength. Because of the greatly reduced melt depth, some of the single-use instruments used in past tests were omitted for this one. The TCs that would measure the interface temperature between the melt and MgO liner (TIW in previous tests) were omitted because they would all be above the level of the melt and therefore irrelevant. The heat flux meters that would normally be installed in the liner and basemat are also omitted. Their purpose is to estimate lateral heat losses and therefore reduce uncertainty in the measured dryout heat flux. However, the greatly reduced melt depth makes it difficult to detect dryout heat flux and so the heat flux meters would be of limited utility.

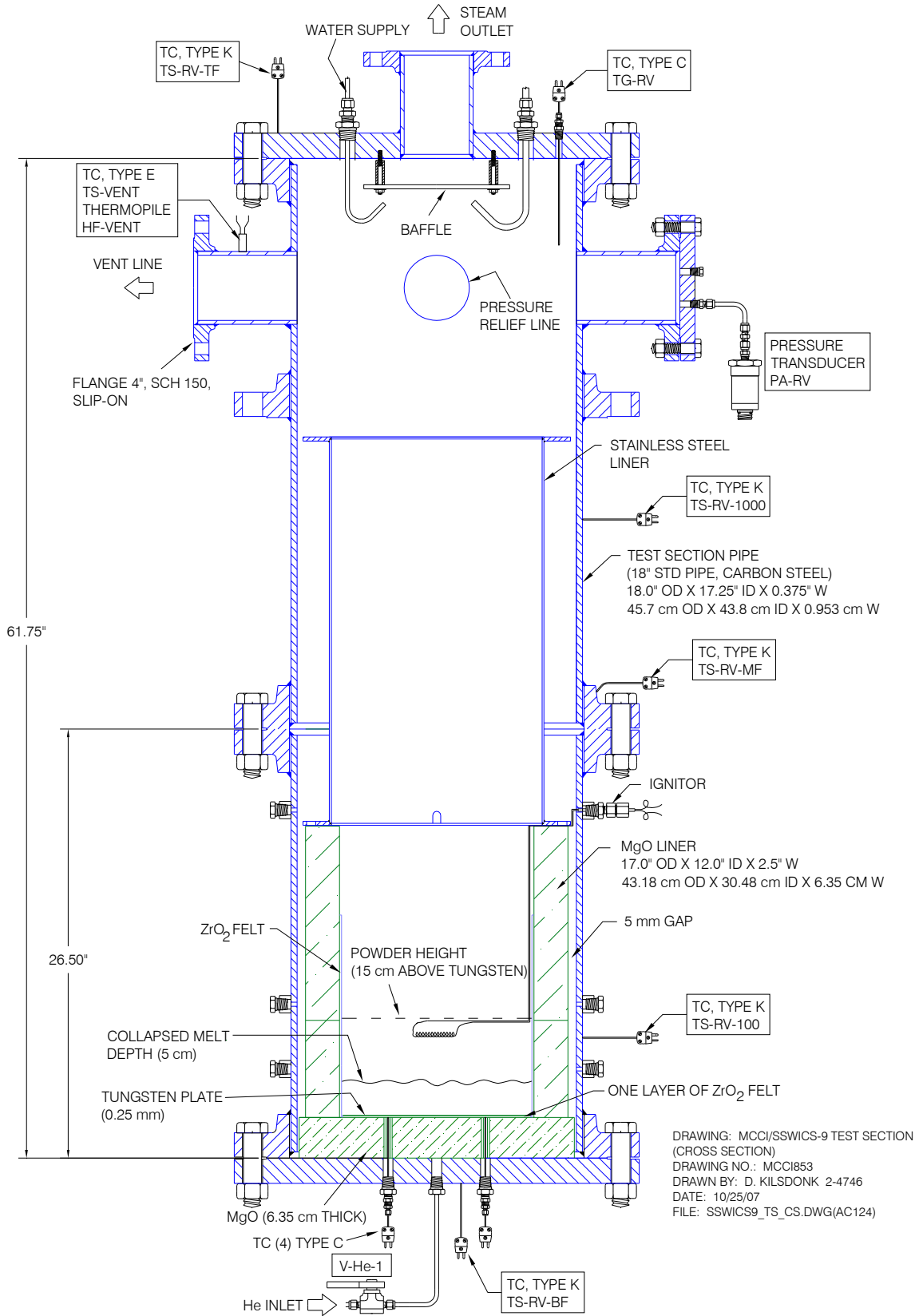


Figure 2.1 Side view of reaction vessel.

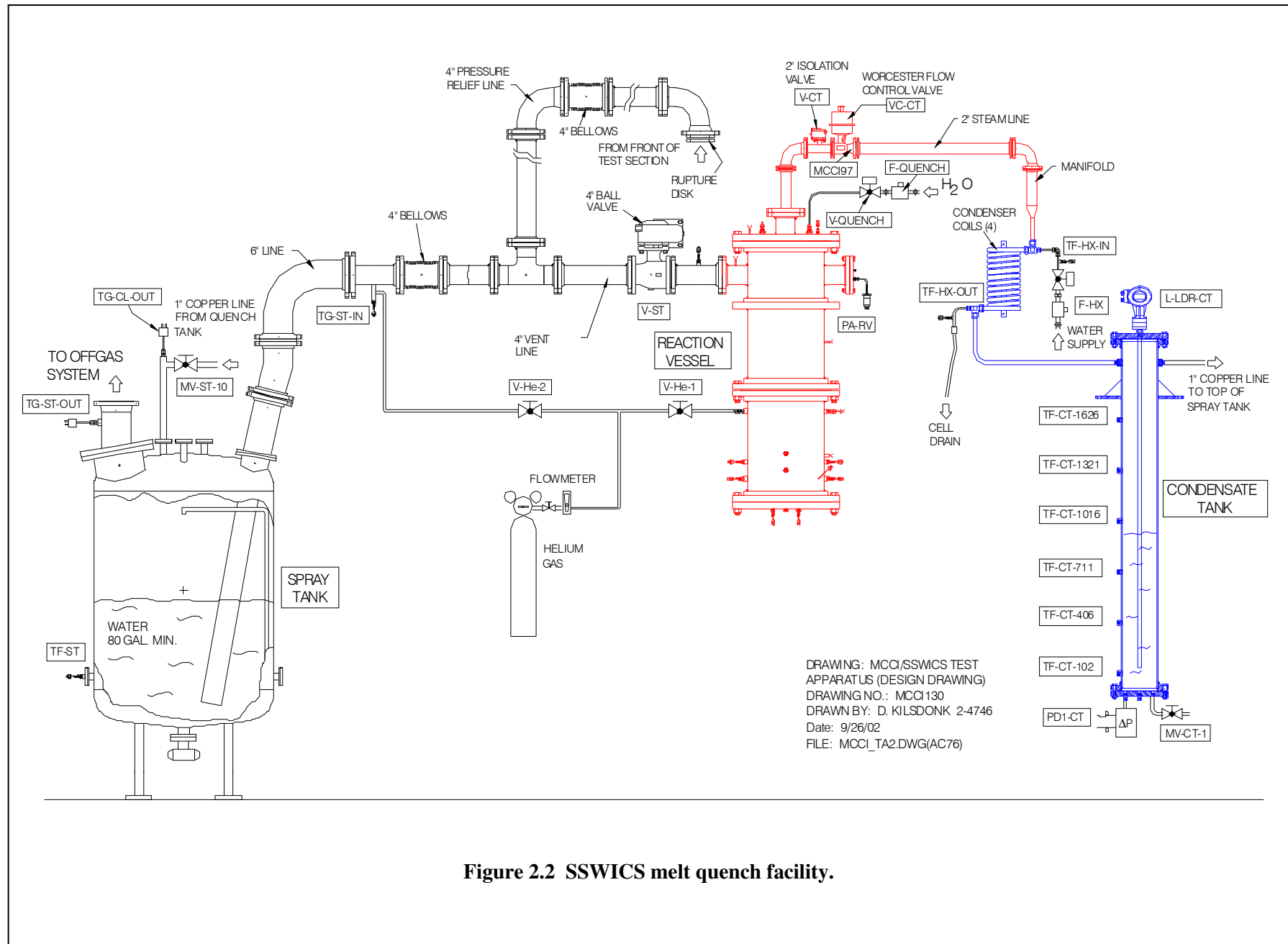


Figure 2.2 SSWICS melt quench facility.

This test employed all the instrumentation used in prior tests to measure the melt cooling rate. The critical measurement in this regard is the steaming rate in the RV, which is found indirectly by measuring the rate of condensate collection in the CT. The condensate inventory is measured with a differential pressure sensor, PD-CT, and a time domain reflectometer, L-TDR-CT.

The remaining instrumentation provides supplementary information to further characterize the test conditions. The nomenclature used to identify thermocouples is as follows: TM (temperature within the corium melt), TF (fluid temperature), TG (gas space temperature), TS (structure temperature), H# (height above the bottom of the melt, in mm, and $\phi\#$ (angle relative to direction north, in degrees). For example, TM-H0- ϕ 180 is located at the bottom of the melt and south of the RV axis.

Four single-junction, tantalum-sheathed TCs are used to measure the melt/MgO basemat interface temperature. Temperatures within the melt itself were measured in previous tests with a multi-junction TC protected by a thermowell, but it was omitted for this test since it can be difficult to remove and it creates a hole in the ingot that could compromise the strength measurement. The TCs are positioned as shown in Fig. 2.3 with the tips above the surface of the melt and in contact with the bottom of the melt. The melt is considered quenched when all four TCs reach the saturation temperature, and this is the basis for terminating the test. Tables 2.1 and 2.2 list the sensors and major valves, respectively.

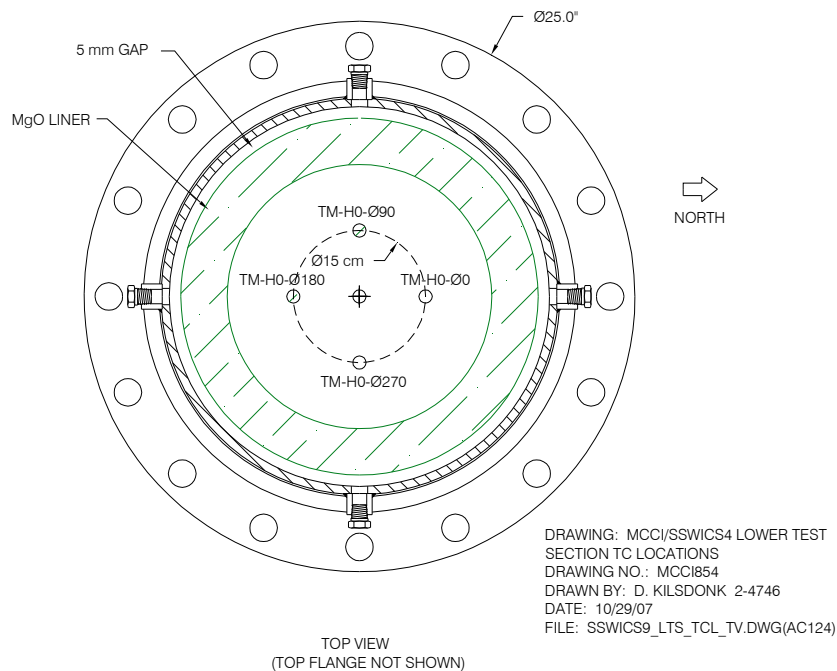


Figure 2.3 Reaction vessel thermocouple locations.

OECD/MCCI-2008-TR02 Rev. 1

#	Channel	Name	Type	Description	Serial #	Output	Range	Accuracy
0	HPS-0	T-CJ-HPS	AD592 IC	Cold junction compensation sensor.	-	1 μ A/K	0-70°C	$\pm 0.5^\circ\text{C}$
1	HPS-1	TM-H0- Φ 0	TC type C	Temperature at interface between bottom of melt and basemat	-	0-37 mV	0-2320°C	$\pm 4.5^\circ\text{C}$ or 1%
2	HPS-2	TM-H90- Φ 0	TC type C	Temperature at interface between bottom of melt and basemat	-	0-37 mV	0-2320°C	$\pm 4.5^\circ\text{C}$ or 1%
3	HPS-3	TM-H180- Φ 0	TC type C	Temperature at interface between bottom of melt and basemat	-	0-37 mV	0-2320°C	$\pm 4.5^\circ\text{C}$ or 1%
4	HPS-4	TM-H270- Φ 0	TC type C	Temperature at interface between bottom of melt and basemat	-	0-37 mV	0-2320°C	$\pm 4.5^\circ\text{C}$ or 1%
5	HPS-5	TG-RV	TC type C	Gas temp. in reaction vessel upper plenum.	-	0-37 mV	0-2320°C	$\pm 4.5^\circ\text{C}$ or 1%
6	HPS-6	Reserve	TC type C	-	-	0-37 mV	0-2320°C	$\pm 4.5^\circ\text{C}$ or 1%
7	HPS-7	Reserve	TC type C	-	-	0-37 mV	0-2320°C	$\pm 4.5^\circ\text{C}$ or 1%
8	HPS-8	Reserve	TC type C	-	-	0-37 mV	0-2320°C	$\pm 4.5^\circ\text{C}$ or 1%
9	HPS-9	Reserve	TC type C	-	-	0-37 mV	0-2320°C	$\pm 4.5^\circ\text{C}$ or 1%
10	HPS-10	Reserve	TC type C	-	-	0-37 mV	0-2320°C	$\pm 4.5^\circ\text{C}$ or 1%
11	HPS-11	Reserve	TC type C	-	-	0-37 mV	0-2320°C	$\pm 4.5^\circ\text{C}$ or 1%
12	HPS-12	Reserve	TC type C	-	-	0-37 mV	0-2320°C	$\pm 4.5^\circ\text{C}$ or 1%
13	HPS-13	Reserve	TC type C	-	-	0-37 mV	0-2320°C	$\pm 4.5^\circ\text{C}$ or 1%
14	HPS-14	Reserve	TC type C	-	-	0-37 mV	0-2320°C	$\pm 4.5^\circ\text{C}$ or 1%
15	HPS-15	Reserve	TC type C	-	-	0-37 mV	0-2320°C	$\pm 4.5^\circ\text{C}$ or 1%
16	HPS-16	Reserve	TC type C	-	-	0-37 mV	0-2320°C	$\pm 4.5^\circ\text{C}$ or 1%
17	HPS-17	Reserve	TC type C	-	-	0-37 mV	0-2320°C	$\pm 4.5^\circ\text{C}$ or 1%
18	HPS-18	Reserve	TC type C	-	-	0-37 mV	0-2320°C	$\pm 4.5^\circ\text{C}$ or 1%
19	HPS-19	Reserve	TC type K	-	-	0-50 mV	0-1250°C	$\pm 2.2^\circ\text{C}$ or 0.75%
20	HPS-20	Reserve	TC type K	-	-	0-50 mV	0-1250°C	$\pm 2.2^\circ\text{C}$ or 0.75%
21	HPS-21	Reserve	TC type K	-	-	0-50 mV	0-1250°C	$\pm 2.2^\circ\text{C}$ or 0.75%
22	HPS-22	TS-RV-tf	TC type K	Temperature of RV top flange.	-	0-50 mV	0-1250°C	$\pm 2.2^\circ\text{C}$ or 0.75%
23	HPS-23	TS-RV-1000	TC type K	Outer wall temp. of RV 1000 mm above bottom of melt.	-	0-50 mV	0-1250°C	$\pm 2.2^\circ\text{C}$ or 0.75%
24	HPS-24	TS-RV-mf	TC type K	Temperature of RV middle flange.	-	0-50 mV	0-1250°C	$\pm 2.2^\circ\text{C}$ or 0.75%
25	HPS-25	TS-RV-100	TC type K	Outer wall temp. of RV 100 mm above bottom of melt.	-	0-50 mV	0-1250°C	$\pm 2.2^\circ\text{C}$ or 0.75%
26	HPS-26	TS-RV-bf	TC type K	Temperature of RV bottom flange.	-	0-50 mV	0-1250°C	$\pm 2.2^\circ\text{C}$ or 0.75%
27	HPS-27	TS-vent	TC type E	Outer wall temp. of vent line.	-	0-70 mV	0-900°C	$\pm 1.7^\circ\text{C}$ or 0.5%
28	HPS-28	TF-CT-102	TC type K	Fluid temp. in condensate tank at a water level of 102 mm.	-	0-50 mV	0-1250°C	$\pm 2.2^\circ\text{C}$ or 0.75%
29	HPS-29	TF-CT-406	TC type K	Fluid temp. in condensate tank at a water level of 406 mm.	-	0-50 mV	0-1250°C	$\pm 2.2^\circ\text{C}$ or 0.75%
30	HPS-30	TF-CT-711	TC type K	Fluid temp. in condensate tank at a water level of 711 mm.	-	0-50 mV	0-1250°C	$\pm 2.2^\circ\text{C}$ or 0.75%
31	HPS-31	TF-CT-1016	TC type K	Fluid temp. in condensate tank at a water level of 1016 mm.	-	0-50 mV	0-1250°C	$\pm 2.2^\circ\text{C}$ or 0.75%
32	HPS-32	TF-CT-1321	TC type K	Fluid temp. in condensate tank at a water level of 1321 mm.	-	0-50 mV	0-1250°C	$\pm 2.2^\circ\text{C}$ or 0.75%
33	HPS-33	TF-CT-1626	TC type K	Fluid temp. in condensate tank at a water level of 1626 mm.	-	0-50 mV	0-1250°C	$\pm 2.2^\circ\text{C}$ or 0.75%
34	HPS-34	TF-HX-in	TC type K	Fluid temp. at HX coolant inlet.	-	0-50 mV	0-1250°C	$\pm 2.2^\circ\text{C}$ or 0.75%
35	HPS-35	TF-HX-out	TC type K	Fluid temp. at HX coolant outlet.	-	0-50 mV	0-1250°C	$\pm 2.2^\circ\text{C}$ or 0.75%
36	HPS-36	HF-vent	Thermopile	Heat Flux through connecting line to V-ST.	0632	0-5.50 mV	0-5 kW/m ²	$\pm 3\%$

Table 2.1 Instrumentation list (part 1 of 2).

OECD/MCCI-2008-TR02 Rev. 1

37	HPS-37	I-ign	DC supply	Current supply for thermite ignitor.	-	0-100 mV	0-25 Amps	-
38	HPS-38	TF-quench	TC type K	Temperature of water injected into RV	-	0-50 mV	0-1250°C	±2.2°C or 0.75%
39	HPS-39	Reserve	-	-	-	-	-	-
40	HPS-40	PA-RV	1810AZ	Absolute pressure in reaction vessel.	02351-00P1PM	1-6 V	0-14 bar gage	±0.14 bar
41	HPS-41	PD-CT	1801DZ	≅P transmitter to measure condensate inventory.	D-3	0-13 V	0-0.35 bar	±0.004 bar
42	HPS-42	L-TDR-CT	BM100A	Time domain reflectometer to measure CT level.	A02331879A	4 - 20 mA	0 - 2 m	±3 mm
43	HPS-43	VDC-P-supply	-	Voltage of the power supply for the pressure transmitters.	-	0 - 15 V	-	-
44	HPS-44	Reserve	-	-	-	-	-	-
45	HPS-45	Reserve	-	-	-	-	-	-
46	HPS-46	Reserve	-	-	-	-	-	-
47	HPS-47	Reserve	-	-	-	-	-	-
48	HPS-48	Reserve	-	-	-	0-40 mV	0-3 MW/m ²	±5%
49	HPS-49	Reserve	-	-	-	0-40 mV	0-3 MW/m ²	±5%
50	HPS-50	Reserve	-	-	-	0-40 mV	0-3 MW/m ²	±5%
51	HPS-51	Reserve	-	-	-	0-40 mV	0-3 MW/m ²	±5%
52	HPS-52	Reserve	-	-	-	0-40 mV	0-3 MW/m ²	±5%
53	HPS-53	Reserve	-	-	-	0-40 mV	0-3 MW/m ²	±5%
54	HPS-54	Reserve	-	-	-	0-50 mV	0-1250°C	±2.2°C or 0.75%
55	HPS-55	Reserve	-	-	-	0-50 mV	0-1250°C	±2.2°C or 0.75%
56	HPS-56	Reserve	-	-	-	0-50 mV	0-1250°C	±2.2°C or 0.75%
57	HPS-57	Reserve	-	-	-	0-50 mV	0-1250°C	±2.2°C or 0.75%
58	HPS-58	Reserve	-	-	-	0-50 mV	0-1250°C	±2.2°C or 0.75%
59	HPS-59	Reserve	-	-	-	0-50 mV	0-1250°C	±2.2°C or 0.75%
60	HPQ-50	T-CJ-HPQ	AD592 IC	Cold junction compensation sensor.	-	1 µA/K	0-70°C	±0.5°C
61	HPQ-51	TF-ST	TC type K	Fluid temp. in spray tank.	-	0-50 mV	0-1250°C	±2.2°C or 0.75%
62	HPQ-52	TG-CL-out	TC type K	Gas temperature in condensate tank outlet line to spray tank.	-	0-50 mV	0-1250°C	±2.2°C or 0.75%
63	HPQ-53	TG-ST-in	TC type K	Gas temp. in the spray tank line inlet.	-	0-50 mV	0-1250°C	±2.2°C or 0.75%
64	HPQ-54	TG-ST-out	TC type K	Gas temp. in the spray tank line outlet.	-	0-50 mV	0-1250°C	±2.2°C or 0.75%
65	HPQ-55	F-quench	Paddlewheel	Flow rate of water into reaction vessel (for quenching melt).	3144	0-5 V	0-50 gpm	±0.5 gpm
66	HPQ-56	F-HX	Paddlewheel	Flow rate of cold water to heat exchangers.	3143	0-5 V	0-50 gpm	±0.5 gpm

Table 2.2 Instrumentation list (part 2 of 2).

Table 2.3 Remotely operated valves.

LabVIEW Channel #	Valve Name	Type	Description	Actuator
1	V-CT	Ball valve	Valve on steam line between reaction vessel and quench tank.	Pneumatic
2	V-quench	Ball valve	Valve on quench water supply line into reaction vessel.	Solenoid
3	V-quench-i	Ball valve	Isolation valve on quench water supply line into reaction vessel.	Solenoid
4	V-quench-b	Ball valve	Valve on back-up quench water supply.	Solenoid
5	V-ST	Ball valve	Valve on vent line between reaction vessel and spray tank.	Pneumatic
Panel	V-HX	Ball valve	Valve on cooling-water line to heat exchangers.	Solenoid
Panel	VC-CT	Ball valve	Control valve on steam line between reaction vessel and quench tank.	Electric

3. Test Parameters and Course of Test

The corium composition for this test is given in Table 3.1 and the general specifications for all nine completed tests are listed in Table 3.2. The 25 kg charge was selected to produce an approximate melt depth of 5 cm.

The facility was heated over the course of a couple of hours to bring the structure temperatures up to about 100°C. During this period the water used for melt quenching was preheated to about 95°C. The preheating is used to reduce the amount of energy absorbed by heat sinks in the early stages of the test. This maximizes the amount of steam reaching the heat exchanger and reduces corrections to the measured corium heat flux.

The igniter coil was energized to initiate thermite ignition, which was first detected by a sudden rise in the upper plenum gas temperature TG-RV. Thermocouples below the melt began rising about fifteen seconds later. The signal from the igniter has not been included in any graph in this report. All data has been plotted so that the x-axis origin corresponds with the initial rise in TG-RV.

The melt thermocouples (TM-H0-φ0 through TM-H0-φ270) reached peak temperatures in the range of roughly 700-1000°C (Fig. A.1). The peaks are lower than those observed in previous tests because the thermocouple tips for this test are flush with the melt rather than protruding into it. Though there is no measurement of temperature near the central region of the melt, it is reasonable to assume that the peak temperature is similar to that of SSWICS-2 (~2100°C), which had the same corium composition. Moreover, a post test examination of the quenched corium confirms that it formed a solid ingot, which also suggests that the peak temperature was near 2000°C.

The next phase of the experiment was the initial quench of the melt. Valve V-CT was opened 65 s after ignition so that steam would be able to travel to the heat exchangers. Valve V-ST was closed shortly thereafter to isolate the vent line and spray tank from the system. Water injection was initiated at 105 s at an average flow rate of 9 l/min, lasting for ~3 minutes (ending at 205 s) and resulting in an integrated flow of approximately 29 liters.

The melt thermocouples reached the saturation temperature after an elapsed time of approximately 24 minutes. The test was subsequently terminated.

Tables 3.1 Corium powder charge and reaction product mass fractions.

Constituent	Mass (kg)
U ₃ O ₈	15.85
CrO ₃	2.84
CaO	0.31
Zr	4.63
Mg	0.01
Si	0.25
SiO ₂	1.06
Al	0.05
Total	25.0

Constituent	Wt %	
	Reactant	Product
U ₃ O ₈	63.38	-
UO ₂	-	60.97
Zr	18.53	-
ZrO ₂	-	25.04
Si	1.00	-
SiO ₂	4.23	6.38
Mg	0.04	-
MgO	-	0.07
Al	0.20	-
Al ₂ O ₃	-	0.38
CaO	1.25	1.25
CrO ₃	11.37	-
Cr	-	5.91

4. Sensor Malfunctions and Abnormalities

Post test examination of the test apparatus and a preliminary review of the data indicate the following:

- 1) The upper and middle flanges were overheated during the preheat stage. At the time of thermite ignition, the top and middle flange temperatures were about 111°C and 124°C, respectively. Cooling of the flanges to the steam saturation temperature contributed to the apparent melt heat flux during the early portion of the transient. This effect, however, is greatly diminished by t=1500 s, which is the point in time that has been used in all past tests for the evaluation of the dryout heat flux.
- 2) Post test disassembly revealed an ingot that was partially bonded with the liner. Though the ingot shifts within the liner, it does not separate from it as did the ingot from SSWICS-9.

5. Data Reduction

Some simple calculations have been performed to provide a preliminary assessment of the test data. The first is a calculation of the coolant inventory in the RV as a function of time. The inventory is the difference between the total amount of liquid injected and the amount boiled off and collected in the CT:

$$M_{H_2O-RV} = \sum_{t=0}^{t=t_{end}} \rho \dot{V} \Delta t - \frac{\pi D^2 \Delta P}{4g} \quad (5.1)$$

where data from sensor F-quench is used for the volumetric flow rate \dot{V} and the liquid density ρ is taken to be 998 kg/m³. The condensate inventory is calculated with readings from sensor PD-CT (ΔP) and the tank diameter D of 0.203 m. Figure A.9 shows both the integrated mass flow

Table 3.2 Test specifications for completed SSWICS experiments.

Parameter	Test Number									
	1	2	3	4	5	6	7	8	9	10
Melt composition (wt% UO ₂ /ZrO ₂ /Cr/Concrete)	61/25/6/8	61/25/6/8	61/25/6/8	48/20/9/23	56/23/7/14	56/23/6/14	64/26/6/4	56/23/6/14	56/23/6/14	61/25/6/8
Concrete type	LCS	SIL	LCS	LCS	LCS	SIL	LCS	SIL	SIL	SIL
Melt mass (kg)	75	75	75	60	68	68	80	68	23	25
Melt depth (cm)	15	15	15	15	15	15	15	15	5	5
Initial Melt Temperature (°C)	~2300	~2100	~2100	~2100	~2100	~1950	~2100	~1900	-	-
System pressure (bar)	1	1	4	4	4	1	4	1	1	1
Water injection flowrate (lpm)	4	4	12	13	6	14	13	10	9	9
Water injected (liters)	33	39	34	40	61	47	40	41	20	29
Test date (day/mo/year)	30/08/02	17/09/02	30/01/03	13/03/03	15/10/03	24/02/04	14/12/04	25/01/07	14/02/08	5/03/08

and CT inventory, labeled F-integrated and M-CT, respectively. The calculated net coolant inventory, denoted M-RV, confirms that the corium was always covered with water.

The corium heat flux was calculated using two different methods. The first considers the rate of condensate collection, which is a measure of the steam flow rate from the RV. Accurate determination of the heat flux at the corium surface must, however, account for various heat sinks. During the injection phase, energy is absorbed raising the coolant to the saturation temperature. Some of the vapor produced by the quenching melt condenses on the walls of the upper plenum to heat the RV structures to the saturation temperature. Later, heat losses from the upper plenum generate continued condensation. Accounting for these heat sinks, the rate of energy transfer through the corium surface is written as:

$$Q = M_{RV} c_p \frac{\partial T}{\partial t} + \dot{m} h_{fg} + [M_S c_M \frac{\partial T}{\partial t} + Q_{HL}] \Big|_{up} \quad (5.2)$$

where \dot{m} is mass flow rate of condensate into the CT, M_S is the mass of the RV upper plenum structures, c_M is their heat capacity, and Q_{HL} represents total upper plenum heat losses. For this report, liquid subcooling has been neglected (an accurate assumption after the injection phase) along with heat losses and time variations in structure temperatures. The condensation rate is calculated from the time derivative of the differential pressure signal PD-CT. The heat transfer rate from the corium is then:

$$Q = \frac{1}{g} \frac{\pi}{4} D^2 \frac{\partial \Delta P}{\partial t} h_{fg} \quad (5.3)$$

where D is again the inner diameter of the CT and the heat of vaporization h_{fg} is 2256 kJ/kg^oC (TG-RV registered 100^oC through most of the transient). The heat flux is obtained by scaling Q with the initial surface area of the corium (0.071 m²). The derivative was calculated with pairs of averaged ΔP readings (an average of 5 measurements at 0.5 Hz) centered around a Δt of 60 s. The averaging and length of Δt were necessary to reduce oscillations in the calculated heat flux.

The second method of calculating corium heat flux uses an energy balance on the secondary side of the heat exchanger. The measured parameters are the coolant flow rate on the secondary side of the cooling coils and the inlet and outlet coolant temperatures. The cooling power of the heat exchanger is then:

$$Q_{HX} = \rho \dot{V}_{HX} c_p (T_{out} - T_{in}) \quad (5.4)$$

where readings from sensors TF-HX-in and TF-HX-out were used for temperatures T_{in} , and T_{out} , respectively. Data from the flow meter F-HX was used for \dot{V}_{HX} while the density and heat capacity of water were taken to be 982 kg/m³ and 4.18 kJ/kg^oC, respectively.

The cooling power of the heat exchanger is related to the steam flow rate out of the RV by the following:

$$Q_{HX} = \dot{m} [h_{fg} + c_p (T_{sat} - T_{con})] \quad (5.5)$$

where \dot{m} is the mass flow rate of steam into the heat exchanger (identical to the flow rate of condensate into the CT, as defined in equation 5.2). From equation 5.5 it can be seen that if

condensate leaves the heat exchanger at the saturation temperature, i.e., there is no subcooling, the cooling power of the heat exchanger is equal to the product of \dot{m} and h_{fg} . In this case, according to equation 5.2, the cooling power of the heat exchanger equals the heat transfer rate from the melt. However, the condensate does not, in general, leave the heat exchanger at the saturation temperature. The result of this subcooling is an overestimation of the corium heat flux when using equation 5.5 and the assumption of $T_{sat} = T_{con}$ (as plotted in figure A.14).

The corium heat flux could be calculated more accurately with the heat exchanger energy balance through the addition of a condensate temperature measurement at the heat exchanger outlet. However, the calculation would still require the steam mass flow rate, which would be derived from the CT level measurements. Thus the heat exchanger energy balance, with the assumption of $T_{sat} = T_{con}$, is considered to be a rough check of the heat flux measurements derived directly from the CT level measurements using equation 5.3.

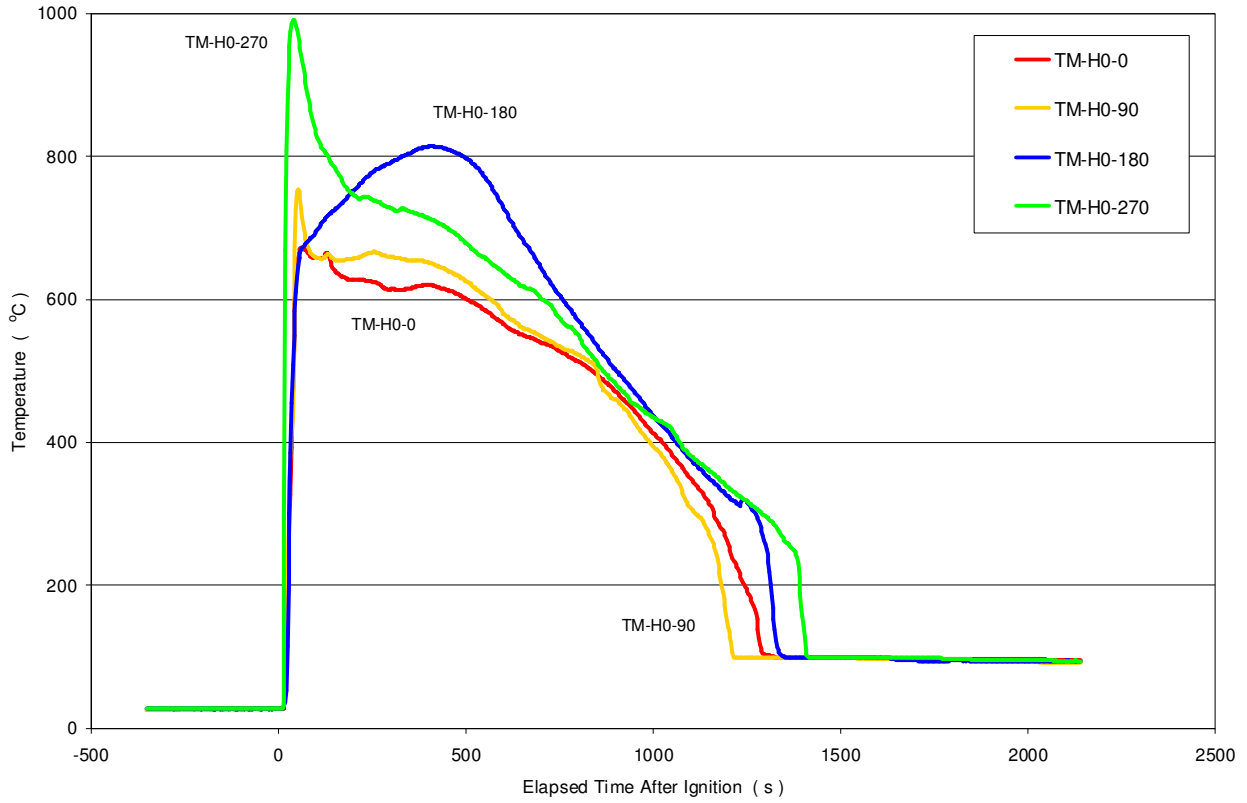
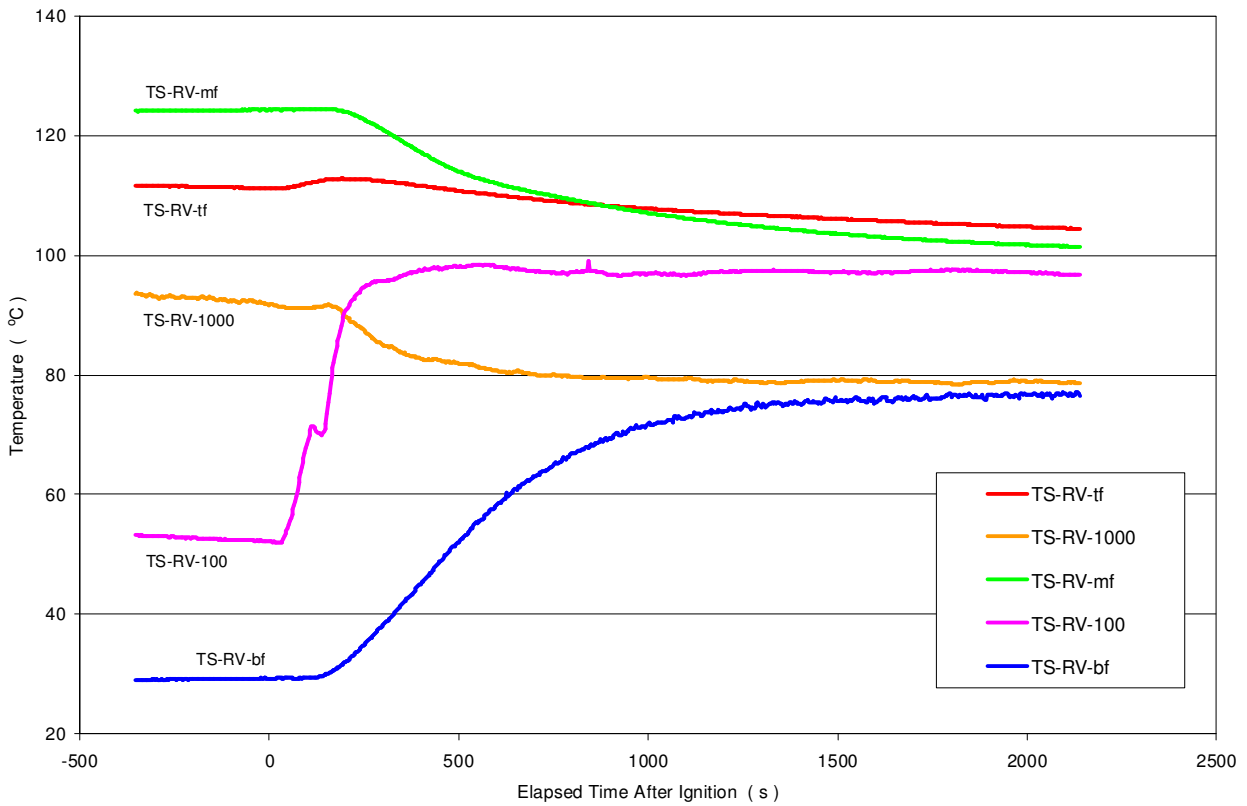
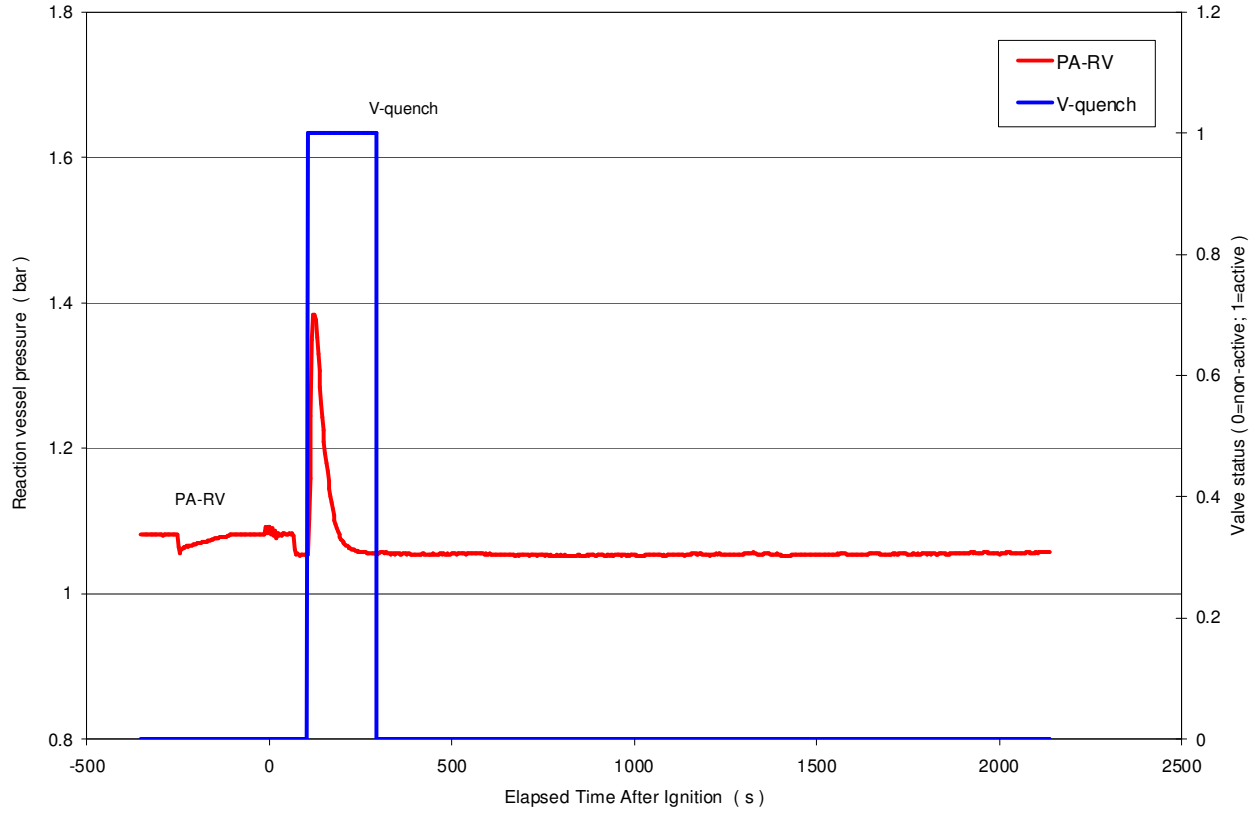
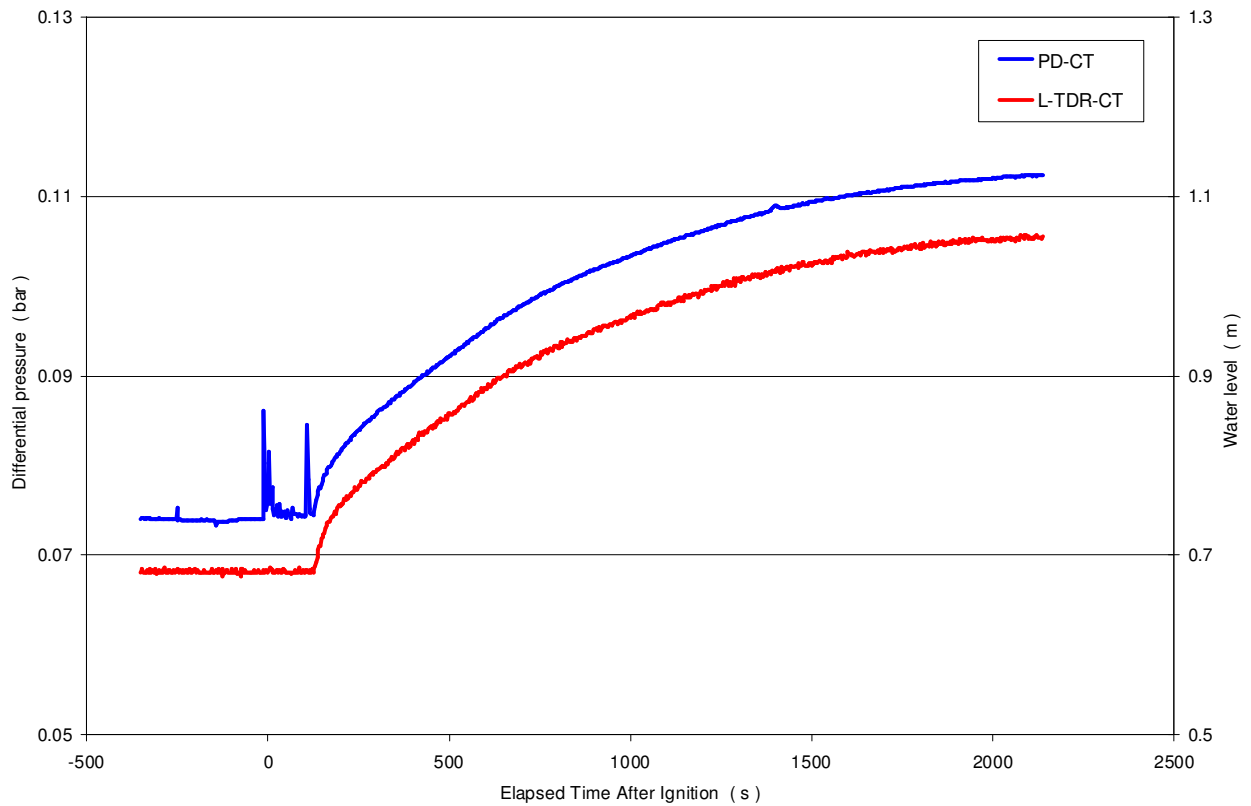


Figure A.1 Temperatures at bottom of melt.
Figure A.2 Temperatures of selected steel structures.





**Figure A.3 Total pressure in reaction vessel and position of valve V-quench.
Figure A.4 Condensate tank inventory as measured by ΔP and level sensors.**



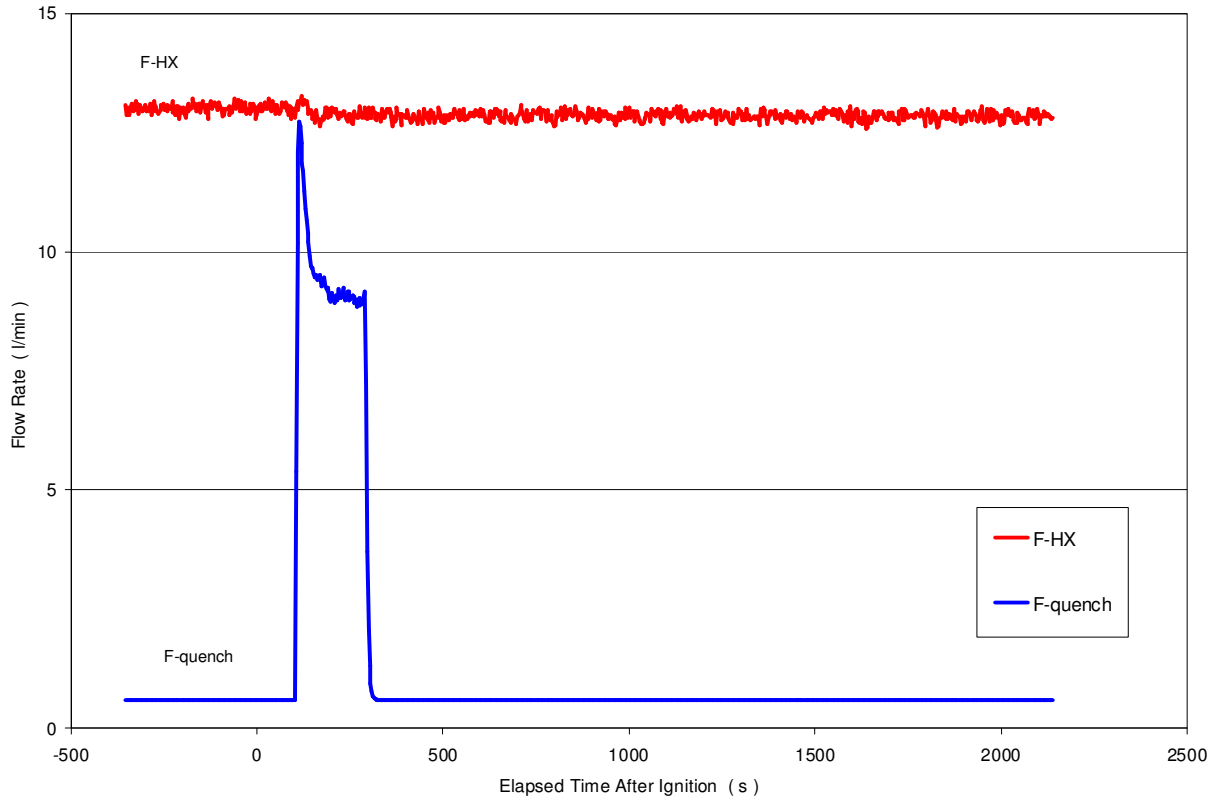
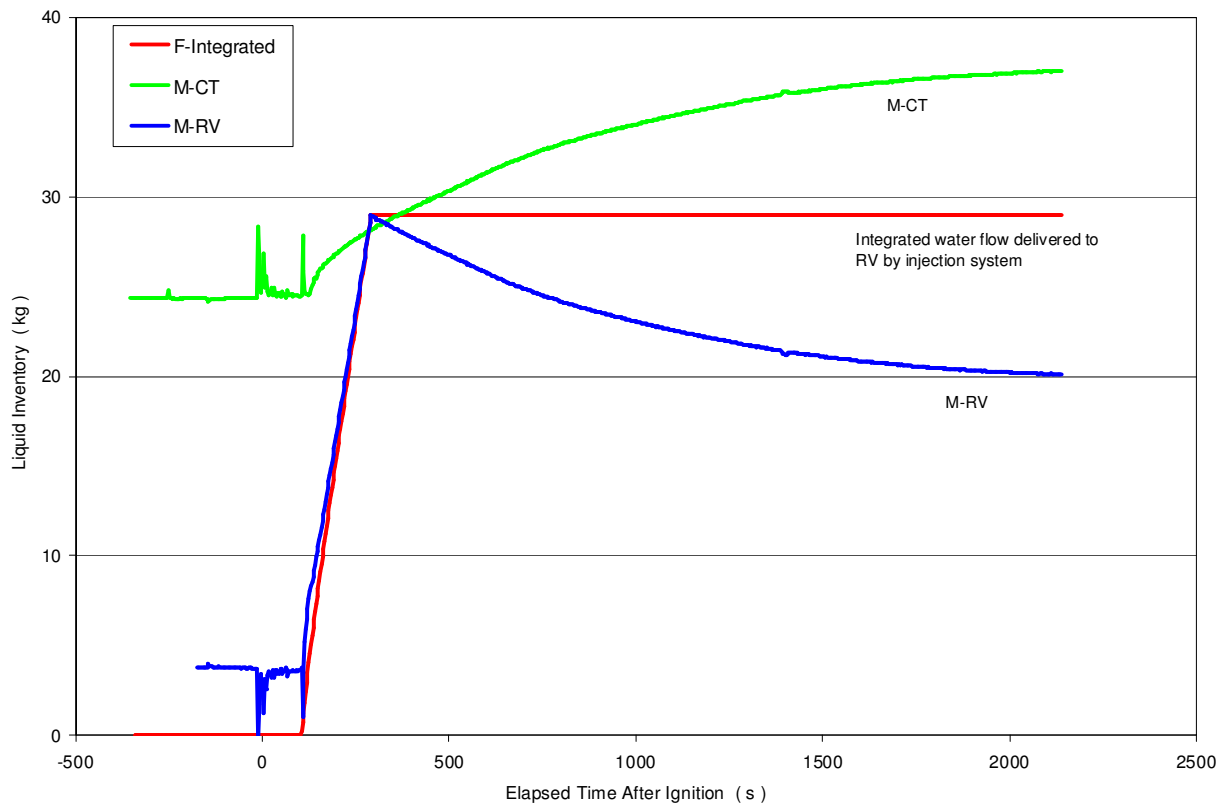


Figure A.5 Water injection into RV and HX secondary side flow rate.
Figure A.6 Integrated quench flow and calculated RV liquid inventory.



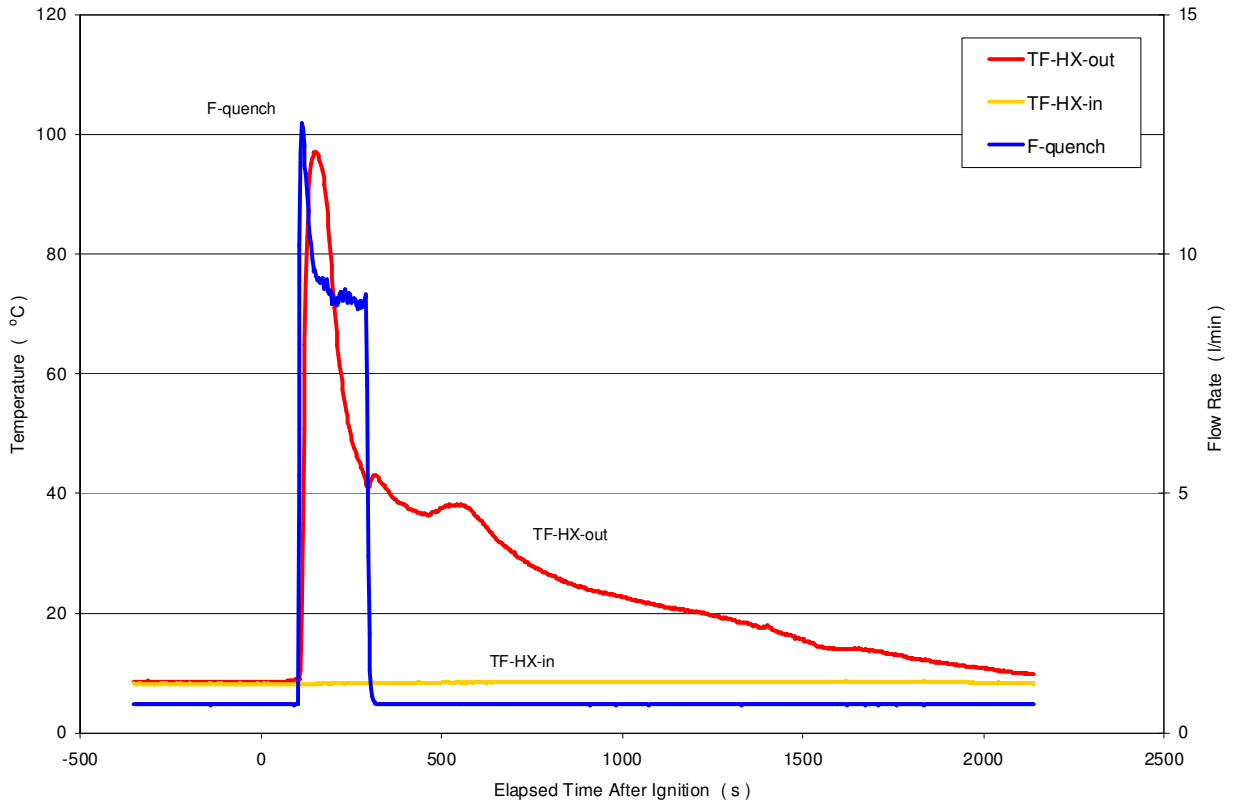
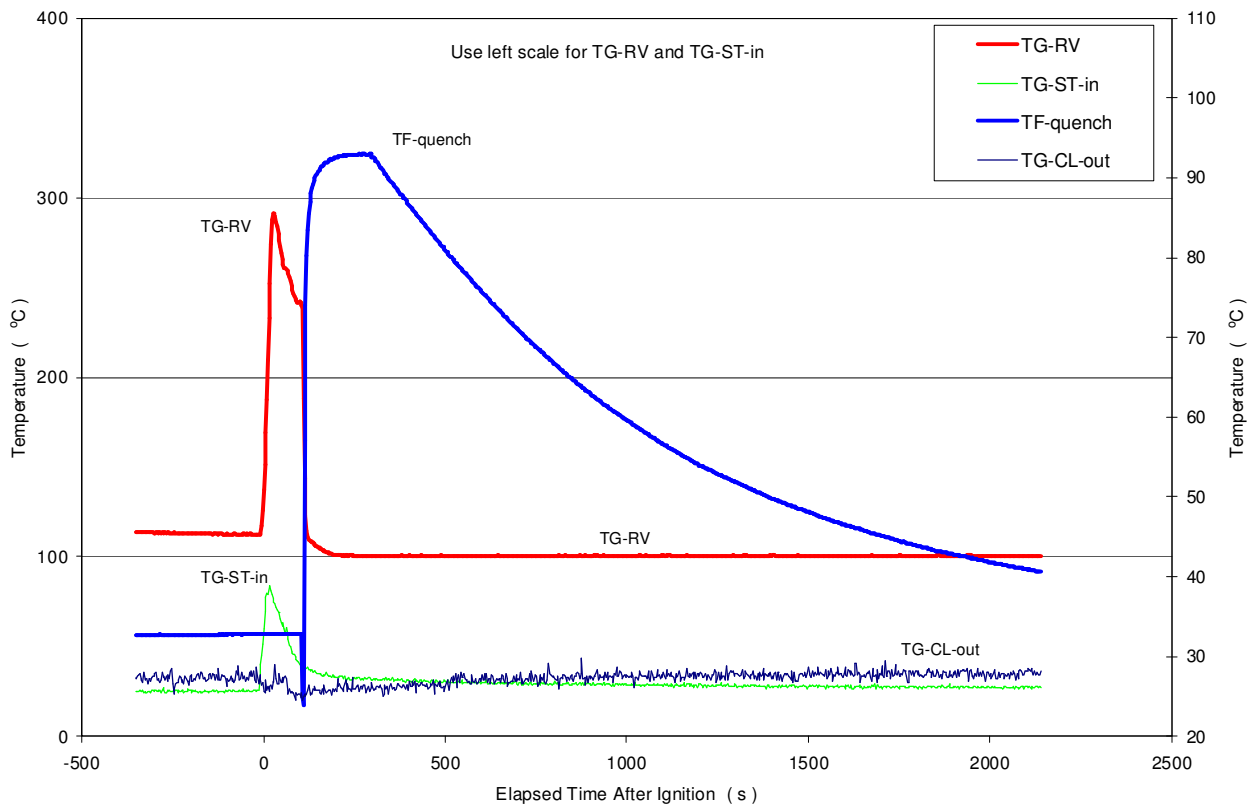


Figure A.7 Secondary side fluid temperatures at HX inlet and outlet.
Figure A.8 Miscellaneous gas and fluid temperatures.



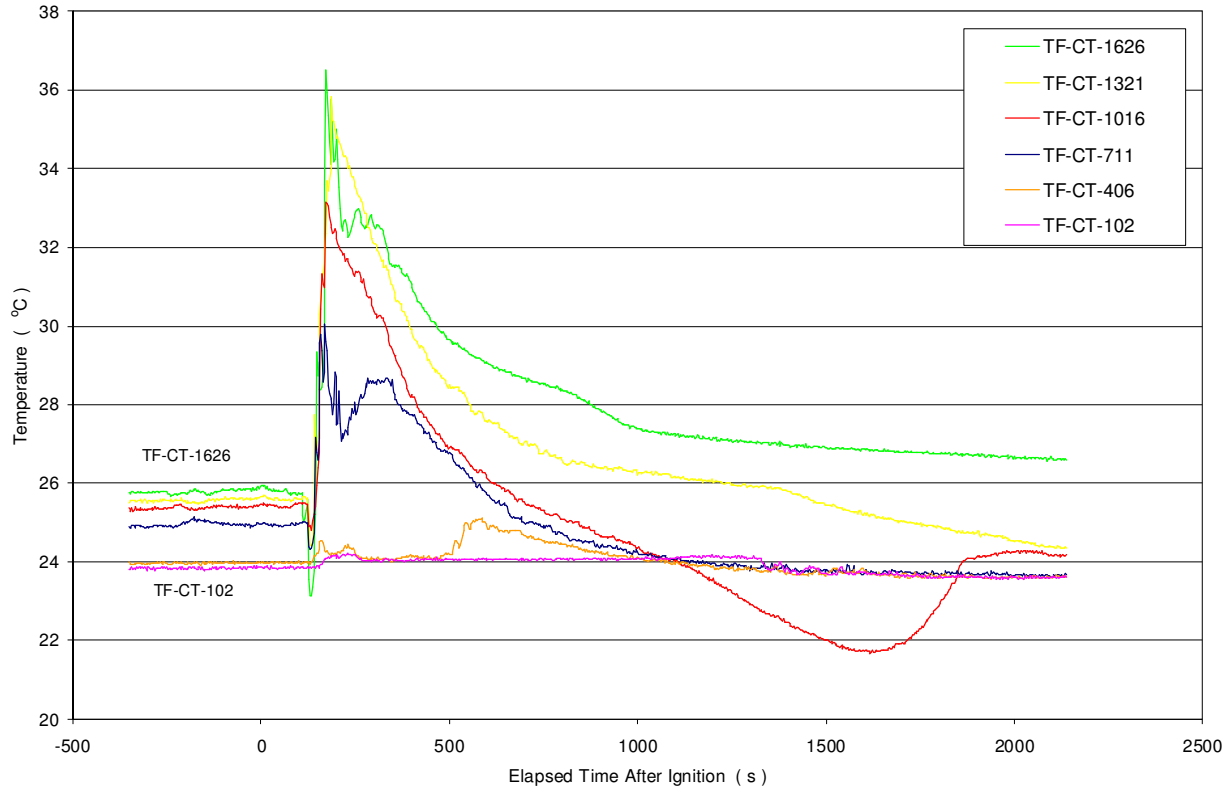


Figure A.9 Fluid temperatures in the condensate tank.
Figure A.10 Heat flux at corium surface based on mass and energy balances.

